

Deep Inelastic Scattering in Improved Lattice QCD

II. The second moment of structure functions^{*}

Giuseppe Beccarini^a, Massimo Bianchi^{b,4}, Stefano Capitani^{a,1,2}
and Giancarlo Rossi^{b,3}

^a*INFN, Sezione di Roma 2, Via della Ricerca Scientifica, I-00133 Roma, Italy*

^b*Dipartimento di Fisica, Università degli Studi di Roma “Tor Vergata”, and
INFN, Sezione di Roma 2, Via della Ricerca Scientifica, I-00133 Roma, Italy*

Abstract

In this paper we present the 1-loop perturbative computation of the renormalization constants and mixing coefficients of the lattice quark operators of rank three whose hadronic elements enter in the determination of the second moment of Deep Inelastic Scattering (DIS) structure functions.

We have employed in our calculations the nearest-neighbor improved “clover-leaf” lattice QCD action. The interest of using this action in Monte Carlo simulations lies in the fact that all terms which in the continuum limit are effectively of order a (a being the lattice spacing) have been demonstrated to be absent from on-shell hadronic lattice matrix elements. We have limited our computations to the quenched case, in which quark operators do not mix with gluon operators.

We have studied the transformation properties under the hypercubic group of the operators up to the rank five (which are related to moments up to the fourth of DIS structure functions), and we discuss the choice of the operators considered in this paper together with the feasibility of lattice computations for operators of higher ranks.

To perform the huge amount of calculations required for the evaluation of all the relevant Feynman diagrams, we have extensively used the symbolic manipulation languages Schoonschip and Form.

1 Introduction

This is the second of two papers addressed to the problem of computing in lattice QCD the 1-loop renormalization constants and mixing coefficients of the operators of rank two and three whose hadronic matrix elements respectively determine the first and second moment of Deep Inelastic Scattering (DIS) structure functions. In the first paper (hereafter referred to as [1]) we have reported the results for the case of the rank two operators. Here we will extend these results to the quark operators of rank three.

Let us start with a brief introduction to light-cone physics and a summary of the improvement program in lattice gauge theories [2–5]. We refer the reader to [1] or to the review paper of Ref. [6] for more details.

1.1 DIS and moments of the structure functions

The quark operators whose matrix elements are related to the moments of the DIS structure functions can be written in the form [7–9]

$$\begin{aligned}
 O_{\{\mu_1 \dots \mu_N\}}^{qS} &= \frac{1}{2^N} \bar{\psi} \gamma_{\{\mu_1} \overleftrightarrow{D}_{\mu_2} \cdots \overleftrightarrow{D}_{\mu_N\}} (1 \pm \gamma_5) \psi \\
 O_{\{\mu_1 \dots \mu_N\}}^{qNS} &= \frac{1}{2^N} \bar{\psi} \gamma_{\{\mu_1} \overleftrightarrow{D}_{\mu_2} \cdots \overleftrightarrow{D}_{\mu_N\}} (1 \pm \gamma_5) \frac{\lambda^f}{2} \psi,
 \end{aligned} \tag{1}$$

where the λ^f 's are flavor matrices. They are gauge invariant, have twist two and are traceless and symmetrized with respect to all Lorentz indices. S and NS superscripts refer to Singlet and Non Singlet flavor structures.

In the unpolarized cross section the γ_5 contributions present in Eqs. (1) average to zero. The other contributions have hadronic matrix elements of the form

$$\langle p | O_{\mu_1 \dots \mu_N}^{(N)} | p \rangle = A_N(\mu) p_{\mu_1} \cdots p_{\mu_N} + \text{trace terms}, \tag{2}$$

* Partially supported by EC Contract ‘‘Computational Particle Physics’’, CHRXCCT92-0051

¹ Address from September 1995: Department of Physics, University of Southampton, Highfield, Southampton SO17 1BJ, United Kingdom

² E-mail: capitani@vxrm70.roma1.infn.it

³ E-mail: rossig@vaxtov.roma2.infn.it

⁴ E-mail: bianchi@vaxtov.roma2.infn.it

where μ is the subtraction point. They contain long distance contributions (non-perturbative physics) and are related to the N -th moment of the DIS structure functions by the equations [10]

$$\langle x_B^N \rangle = \int dx_B x_B^N \mathcal{F}_k(q^2, x_B) = C_{N+1}(q^2/\mu^2) A_{N+1}(\mu). \quad (3)$$

1.2 Improved lattice QCD

The nearest-neighbor improved action (SW “clover-leaf” action) employed in these calculations is obtained by adding to the standard Wilson action [11] the Sheikholeslami–Wohlert [4] nearest-neighbor interaction term⁵

$$\Delta S_1^f = -ig_0 a^4 \sum_{n,\mu\nu} \frac{r}{4a} \bar{\psi}_n \sigma_{\mu\nu} F_{n,\mu\nu} \psi_n. \quad (6)$$

This term modifies the standard order g_0 quark-gluon Wilson vertex,

$$(V)_\rho^{bc}(k, k') = -g_0 (t^A)_{bc} \left[r \sin \frac{a(k+k')_\rho}{2} + i\gamma_\rho \cos \frac{a(k+k')_\rho}{2} \right], \quad (7)$$

by adding to it the extra piece (“improved vertex”)

$$(V^I)_\rho^{bc}(k, k') = -g_0 \frac{r}{2} (t^A)_{bc} \cos \frac{a(k-k')_\rho}{2} \sum_\lambda \sigma_{\rho\lambda} \sin a(k-k')_\lambda, \quad (8)$$

where k and k' are the momenta of the incoming and the outgoing quark respectively and ρ is the Lorentz index carried by the gluon. The quark and gluon propagators, as well as the interaction between the quark current and an even number of gluons, turn out to be unmodified. To the order to which we will perform our calculations we will not need the expression of higher order quark-gluon vertices.

⁵ Here $F_{n,\mu\nu}$ is not the naive lattice “plaquette”

$$P_{n,\mu\nu} = \frac{1}{2ig_0 a^2} (U_{n,\mu\nu} - U_{n,\mu\nu}^+), \quad U_{n,\mu\nu} = U_{n,\mu} U_{n+\mu,\nu} U_{n+\nu,\mu}^+ U_{n,\nu}^+, \quad (4)$$

but rather the average of the four plaquettes lying in the plane $\mu\nu$, stemming from the point n :

$$F_{n,\mu\nu} = \frac{1}{4} \sum_{\mu\nu=\pm} P_{n,\mu\nu} = \frac{1}{8ig_0 a^2} \sum_{\mu\nu=\pm} (U_{n,\mu\nu} - U_{n,\mu\nu}^+). \quad (5)$$

Besides adding the term (6) to the action, for consistency [5] one also has to rotate all the quark fields appearing in Green functions according to the rule (see Appendix A for the definition of the lattice covariant derivatives)

$$\begin{aligned}\psi &\longrightarrow \left(1 - \frac{ar}{2} \overrightarrow{\not{D}}\right) \psi \\ \bar{\psi} &\longrightarrow \bar{\psi} \left(1 + \frac{ar}{2} \overleftarrow{\not{D}}\right).\end{aligned}\tag{9}$$

As it has already been noticed in [1], the transformations (9) are the sources of very many algebraic complications in perturbative calculations.

2 Structure of the operators

In this paper we want to study the lattice renormalization of the rank three quark operator

$$O_{\{\mu\nu\tau\}}^q = \frac{1}{8} \bar{\psi} \gamma_{\{\mu} \overleftrightarrow{D}_{\nu} \overleftrightarrow{D}_{\tau\}} \psi.\tag{10}$$

Its hadronic matrix elements are related to the second moment of the x_B -distribution of quarks inside the hadron. $O_{\{\mu\nu\tau\}}^q$ is the (parity conserving piece of the) second operator in the list given in Eqs. (1).

We will restrict ourselves to the quenched approximation, and consequently we will not have to consider the mixing between the quark operator (10) and the gluon operator $\sum_{\rho} \text{Tr} \left[F_{\{\mu\rho} \overleftrightarrow{D}_{\nu} F_{\rho\tau\}} \right]$. Actually both the experimental and the numerical determinations of the x_B -distribution of gluons are much harder to obtain than the corresponding quantities for quarks.

2.1 General considerations

The explicit expression of the “improved” quark operator, obtained by taking into account the rotations (9) on the fermion fields, is given by

$$\begin{aligned}(O_{\{\mu\nu\tau\}}^q)^{\text{I}} = \\ \frac{1}{8} \left[\bar{\psi} \gamma_{\{\mu} \overrightarrow{D}_{\nu} \overrightarrow{D}_{\tau\}} \psi - \bar{\psi} \gamma_{\{\mu} \overleftarrow{D}_{\nu} \overrightarrow{D}_{\tau\}} \psi - \bar{\psi} \gamma_{\{\mu} \overrightarrow{D}_{\nu} \overleftarrow{D}_{\tau\}} \psi + \bar{\psi} \gamma_{\{\mu} \overleftarrow{D}_{\nu} \overleftarrow{D}_{\tau\}} \psi \right]\end{aligned}$$

$$\begin{aligned}
& -\frac{ar}{16} \left[\bar{\psi} \gamma_{\{\mu} \overrightarrow{D}_\nu \overrightarrow{D}_{\tau\}} \overrightarrow{\not{D}} \psi - \bar{\psi} \gamma_{\{\mu} \overleftarrow{D}_\nu \overrightarrow{D}_{\tau\}} \overrightarrow{\not{D}} \psi \right. \\
& - \bar{\psi} \gamma_{\{\mu} \overrightarrow{D}_\nu \overleftarrow{D}_{\tau\}} \overrightarrow{\not{D}} \psi + \bar{\psi} \gamma_{\{\mu} \overleftarrow{D}_\nu \overleftarrow{D}_{\tau\}} \overrightarrow{\not{D}} \psi - \bar{\psi} \overleftarrow{\not{D}} \gamma_{\{\mu} \overrightarrow{D}_\nu \overrightarrow{D}_{\tau\}} \psi \\
& \left. + \bar{\psi} \overleftarrow{\not{D}} \gamma_{\{\mu} \overleftarrow{D}_\nu \overrightarrow{D}_{\tau\}} \psi + \bar{\psi} \overleftarrow{\not{D}} \gamma_{\{\mu} \overrightarrow{D}_\nu \overleftarrow{D}_{\tau\}} \psi - \bar{\psi} \overleftarrow{\not{D}} \gamma_{\{\mu} \overleftarrow{D}_\nu \overleftarrow{D}_{\tau\}} \psi \right] \\
& -\frac{a^2 r^2}{32} \left[\bar{\psi} \overleftarrow{\not{D}} \gamma_{\{\mu} \overrightarrow{D}_\nu \overrightarrow{D}_{\tau\}} \overrightarrow{\not{D}} \psi - \bar{\psi} \overleftarrow{\not{D}} \gamma_{\{\mu} \overleftarrow{D}_\nu \overrightarrow{D}_{\tau\}} \overrightarrow{\not{D}} \psi \right. \\
& \left. - \bar{\psi} \overleftarrow{\not{D}} \gamma_{\{\mu} \overrightarrow{D}_\nu \overleftarrow{D}_{\tau\}} \overrightarrow{\not{D}} \psi + \bar{\psi} \overleftarrow{\not{D}} \gamma_{\{\mu} \overleftarrow{D}_\nu \overleftarrow{D}_{\tau\}} \overrightarrow{\not{D}} \psi \right]. \tag{11}
\end{aligned}$$

As can be seen, the three-index case introduces a new feature in the expression of improved operators, namely the appearance of the cross-derivative term, $\bar{\psi} \overrightarrow{D}_\mu \overleftarrow{D}_\nu \psi$, which has to be defined according to the formula

$$\begin{aligned}
\bar{\psi}_n \overrightarrow{D}_\mu \overleftarrow{D}_\nu \psi_n &= -\frac{1}{4a^2} \left[\bar{\psi}_{n-\nu} U_{n-\nu,\mu} U_{n+\mu-\nu,\nu} \psi_{n+\mu} - \bar{\psi}_{n+\nu} U_{n+\nu,\mu} U_{n+\mu,\nu}^+ \psi_{n+\mu} \right. \\
& \left. - \bar{\psi}_{n-\nu} U_{n-\mu-\nu,\mu}^+ U_{n-\mu-\nu,\nu} \psi_{n-\mu} + \bar{\psi}_{n+\nu} U_{n-\mu+\nu,\mu}^+ U_{n-\mu,\nu}^+ \psi_{n-\mu} \right]. \tag{12}
\end{aligned}$$

The more usual terms $\bar{\psi} \overrightarrow{D}_\mu \overrightarrow{D}_\nu \psi$, $\bar{\psi} \overleftarrow{D}_\mu \overleftarrow{D}_\nu \psi$ and $\bar{\psi} \overleftarrow{D}_\mu \overrightarrow{D}_\nu \psi$ have respectively the expressions

$$\begin{aligned}
\bar{\psi}_n \overrightarrow{D}_\mu \overrightarrow{D}_\nu \psi_n &= \frac{1}{4a^2} \bar{\psi}_n \left[U_{n,\mu} U_{n+\mu,\nu} \psi_{n+\mu+\nu} - U_{n,\mu} U_{n+\mu-\nu,\nu}^+ \psi_{n+\mu-\nu} \right. \\
& \left. - U_{n-\mu,\mu}^+ U_{n-\mu,\nu} \psi_{n-\mu+\nu} + U_{n-\mu,\mu}^+ U_{n-\mu-\nu,\nu}^+ \psi_{n-\mu-\nu} \right] \tag{13}
\end{aligned}$$

$$\begin{aligned}
\bar{\psi}_n \overleftarrow{D}_\mu \overrightarrow{D}_\nu \psi_n &= -\frac{1}{4a^2} \left[\bar{\psi}_{n-\mu} U_{n-\mu,\mu} U_{n,\nu} \psi_{n+\nu} - \bar{\psi}_{n+\mu} U_{n,\mu}^+ U_{n,\nu} \psi_{n+\nu} \right. \\
& \left. - \bar{\psi}_{n-\mu} U_{n-\mu,\mu} U_{n-\nu,\nu}^+ \psi_{n-\nu} + \bar{\psi}_{n+\mu} U_{n,\mu}^+ U_{n-\nu,\nu}^+ \psi_{n-\nu} \right] \tag{14}
\end{aligned}$$

$$\begin{aligned}
\bar{\psi}_n \overleftarrow{D}_\mu \overleftarrow{D}_\nu \psi_n &= \frac{1}{4a^2} \left[\bar{\psi}_{n+\mu+\nu} U_{n+\nu,\mu}^+ U_{n,\nu}^+ - \bar{\psi}_{n-\mu+\nu} U_{n-\mu+\nu,\mu} U_{n,\nu}^+ \right. \\
& \left. - \bar{\psi}_{n+\mu-\nu} U_{n-\nu,\mu}^+ U_{n-\nu,\nu} + \bar{\psi}_{n-\mu-\nu} U_{n-\mu-\nu,\mu} U_{n-\nu,\nu} \right] \psi_n. \tag{15}
\end{aligned}$$

The requirement that fixes the exact form of the cross-derivative term is that the right-derivative, \overrightarrow{D}_ν , and the corresponding left-derivative, \overleftarrow{D}_ν , should be obtained one from the other by an integration by parts, that amounts on the lattice to a shift of one site in the ν (in this example) direction.

Using the nearest-neighbor improved action, we want to compute to 1-loop in the chiral limit the matrix elements

$$M_{\mu\nu\tau}(p) \equiv \langle p | O_{\mu\nu\tau}^q | p \rangle, \quad (16)$$

where $|p\rangle$ is a one-quark state of momentum p and vanishing (renormalized) mass. The renormalization constants and mixing coefficients of $O_{\mu\nu\tau}^q$ can be extracted from the knowledge of the amplitudes $M_{\mu\nu\tau}(p)$.

2.2 Operator mixing

Lorentz indices in Eq. (16) have to be chosen carefully by looking at the transformation properties of the resulting operators with respect to the hypercubic group, $H(4)$ [12,13]. This group, which consists of the discrete proper rotations (no parity reflections⁶) in four dimensions, is the remnant of the proper euclidean Lorentz group on a discretized space-time.

In moving from a continuum four-dimensional relativistic theory to its lattice version, the proper (euclidean) Lorentz invariance $O(4)$ is broken to the invariance under the proper hypercubic group $H(4)$. For this reason representations that under the $O(4)$ group are irreducible become in general reducible under $H(4)$ when the corresponding operators are written on the lattice. Therefore, some special care must be exerted to avoid unwanted mixings.

The most dangerous situation occurs if one considers the operator $O_{\mu\nu\tau}^q$ with $\mu = \nu = \tau$, because it can mix (and indeed it does) with the lower-dimensional operator

$$\bar{\psi} \gamma_\mu \psi, \quad (17)$$

with a power divergent ($\sim 1/a^2$) mixing coefficient. Any simulation carried out with an operator with three equal indices will require a delicate non-perturbative subtraction of the lower-dimensional operator. This ends up in very large statistical errors in the results of these simulations.

⁶ In the following we will restrict ourselves to the transformation properties of the operators under the proper hypercubic group, as we will only consider unpolarized structure functions, in which case the γ_5 contributions drop out from Eqs. (1).

Another possibility is to take $\mu \neq \nu \neq \tau (\neq \mu)$. In this way one selects an irreducible representation of $H(4)$, and no mixing is anymore allowed. We will take as a typical component of the multiplet of operators transforming according to this representation the operator $O_{\{123\}}^q$. The drawback of choosing $\mu \neq \nu \neq \tau (\neq \mu)$ in a Monte Carlo simulation is that two components of the momentum of the hadron are bound to be different from zero and from each other. This can lead to significant systematical errors coming from the increased sensitivity to the granularity of the lattice.

A third possible choice (and the best one) is $\mu = \nu \neq \tau$. In this case only one component of the hadron momentum has to be taken different from zero. Martinelli and Sachrajda have shown that power divergent subtractions can be avoided by using the particular combination [14,15]

$$O_{\text{DIS}}^q \equiv O_{\{411\}}^q - \frac{1}{2}(O_{\{422\}}^q + O_{\{433\}}^q), \quad (18)$$

which turns out to belong to an irreducible representation of $H(4)$. Using the standard Wilson action, they estimated the renormalization constant of this operator in the hypothesis of tadpole dominance of lattice perturbation theory.

Unfortunately, the fact that the operator (18) belongs to an irreducible representation of $H(4)$ is not enough for it to be multiplicatively renormalizable, because in the decomposition of a rank three tensor into irreducible representations, the representation to which the operator (18) belongs appears more than once. As a consequence, mixing can occur among operators belonging to these equivalent representations.

In the next subsection we will present the complete solution to the problem of decomposing in irreducible $H(4)$ representations the particular tensor products of representations that arise when one considers the (parity conserving pieces of the) DIS quark operators of rank 3, 4 and 5 appearing in Eqs. (1).

2.3 Lattice transformation properties of DIS quark operators

The proper hypercubic group $H(4)$ has 192 elements. Its 13 irreducible representations are listed in Table 1, where an extra subscript is used to label different representations with the same dimension. For example, the representation labelled as $\mathbf{1}_1$ is the identity, while the representation labelled as $\mathbf{1}_2$ is the totally antisymmetric one. In Table 1 we also give the corresponding $O(4)$ representation in $SU(2) \otimes SU(2)$ notation, when it exists. We recall that the representations $\mathbf{3}_5$, $\mathbf{3}_6$ and $\mathbf{4}_2$ can be obtained as tensor product of $\mathbf{1}_2$ with $\mathbf{3}_3$, $\mathbf{3}_4$ and $\mathbf{4}_1$ respectively. With an abuse of notation, in the literature they are often denoted respectively as $(1, 0)$, $(0, 1)$ and $(\frac{1}{2}, \frac{1}{2})$.

Table 1

The irreducible representations of the hypercubic group (the corresponding $O(4)$ representations are also indicated)

$\mathbf{1}_1$	$\mathbf{1}_2$	$\mathbf{2}$	$\mathbf{3}_1$	$\mathbf{3}_2$	$\mathbf{3}_3$	$\mathbf{3}_4$	$\mathbf{3}_5$	$\mathbf{3}_6$	$\mathbf{4}_1$	$\mathbf{4}_2$	$\mathbf{6}$	$\mathbf{8}$
(0,0)	—	—	—	—	(1,0)	(0,1)	—	—	$(\frac{1}{2}, \frac{1}{2})$	—	—	—

Table 2

Multiplet structure for $\mathbf{4}_1 \otimes \mathbf{4}_1 \otimes \mathbf{4}_1$

typical index pattern	multiplets
123	$\mathbf{4}_1 + \mathbf{4}_2 + \mathbf{8} + \mathbf{8}$
112	$3 \cdot (\mathbf{4}_1 + \mathbf{8})$
111	$\mathbf{4}_1$

We are interested in the decomposition of tensor products such as $\mathbf{4}_1 \otimes \mathbf{4}_1 \otimes \dots \otimes \mathbf{4}_1$ to which all the operators listed in Eqs. (1) belong. According to Table 1, the irreducible $\mathbf{4}_1$ representation of $H(4)$ corresponds to the irreducible vector representation $(\frac{1}{2}, \frac{1}{2})$ of $O(4)$.

The case of the rank three operator is easily worked out remembering the corresponding $O(4)$ decomposition formula

$$\left(\frac{1}{2}, \frac{1}{2}\right) \otimes \left(\frac{1}{2}, \frac{1}{2}\right) \otimes \left(\frac{1}{2}, \frac{1}{2}\right) = 4 \cdot \left(\frac{1}{2}, \frac{1}{2}\right) + 2 \cdot \left(\frac{1}{2}, \frac{3}{2}\right) + 2 \cdot \left(\frac{3}{2}, \frac{1}{2}\right) + \left(\frac{3}{2}, \frac{3}{2}\right). \quad (19)$$

One finds for $H(4)$

$$\mathbf{4}_1 \otimes \mathbf{4}_1 \otimes \mathbf{4}_1 = 5 \cdot \mathbf{4}_1 + \mathbf{4}_2 + 5 \cdot \mathbf{8}. \quad (20)$$

These representations can be organized according to the patterns and number of indices having the same value, as shown in Table 2. In the first column we give a typical representative for each type of index pattern.

It is straightforward although tedious to extend the above results to the more complicated cases of operators of rank four and five. The $H(4)$ decomposition of the 256 components of the lattice rank four operator is given by

$$\begin{aligned} \mathbf{4}_1 \otimes \mathbf{4}_1 \otimes \mathbf{4}_1 \otimes \mathbf{4}_1 = & 5 \cdot \mathbf{1}_1 + \mathbf{1}_2 + 5 \cdot \mathbf{2} + 10 \cdot \mathbf{3}_1 + 6 \cdot \mathbf{3}_2 \\ & + 10 \cdot \mathbf{3}_3 + 10 \cdot \mathbf{3}_4 + 6 \cdot \mathbf{3}_5 + 6 \cdot \mathbf{3}_6 + 16 \cdot \mathbf{6}. \end{aligned} \quad (21)$$

The decomposition results in 75 multiplets belonging to ten different types of representations, which again can be organized according to the patterns and number of indices having the same value, as shown in Table 3.

Table 3

Multiplet structure for $\mathbf{4}_1 \otimes \mathbf{4}_1 \otimes \mathbf{4}_1 \otimes \mathbf{4}_1$

typical index pattern	multiplets
1234	$\mathbf{1}_1 + \mathbf{1}_2 + \mathbf{2} + \mathbf{2} + \mathbf{3}_1 + \mathbf{3}_1 + \mathbf{3}_1 + \mathbf{3}_2 + \mathbf{3}_2 + \mathbf{3}_2$
1123	$6 \cdot (\mathbf{3}_3 + \mathbf{3}_4 + \mathbf{3}_5 + \mathbf{3}_6 + \mathbf{6} + \mathbf{6})$
1122	$3 \cdot (\mathbf{1}_1 + \mathbf{2} + \mathbf{3}_1 + \mathbf{3}_1 + \mathbf{3}_2)$
1112	$4 \cdot (\mathbf{3}_3 + \mathbf{3}_4 + \mathbf{6})$
1111	$\mathbf{1}_1 + \mathbf{3}_1$

Table 4

Multiplet structure for $\mathbf{4}_1 \otimes \mathbf{4}_1 \otimes \mathbf{4}_1 \otimes \mathbf{4}_1 \otimes \mathbf{4}_1$

typical index pattern	multiplets
11234	$10 \cdot (\mathbf{4}_1 + \mathbf{4}_2 + \mathbf{8} + \mathbf{8})$
11223	$15 \cdot (\mathbf{4}_1 + \mathbf{4}_2 + \mathbf{8} + \mathbf{8})$
11222	$10 \cdot (\mathbf{4}_1 + \mathbf{8})$
11123	$10 \cdot (\mathbf{4}_1 + \mathbf{4}_2 + \mathbf{8} + \mathbf{8})$
11112	$5 \cdot (\mathbf{4}_1 + \mathbf{8})$
11111	$\mathbf{4}_1$

Finally, the 1024 components of the lattice rank five operator decompose in 171 multiplets of only three different kinds,

$$\mathbf{4}_1 \otimes \mathbf{4}_1 \otimes \mathbf{4}_1 \otimes \mathbf{4}_1 \otimes \mathbf{4}_1 = 51 \cdot \mathbf{4}_1 + 35 \cdot \mathbf{4}_2 + 85 \cdot \mathbf{8}, \quad (22)$$

and their classification is reported in Table 4.

2.4 Choice of the rank three operators

It is easily seen that the operator (18) belongs to the eight-dimensional representation of $H(4)$. Furthermore, we see from Eq. (20) that when one decomposes $O_{\mu\nu\tau}^q$ in $H(4)$ multiplets there arise five eight-dimensional representations. The crucial point here is that the hypercubic group $H(4)$ possesses only one single eight-dimensional irreducible representation (see Table 1). Therefore all the five $\mathbf{8}$'s that come out in the decomposition of the rank three operators into $H(4)$ multiplets can in principle mix among themselves. This is at variance with what happens in the case of the rank two operator, where the operator $O_{\{41\}}^q$ is multiplicatively renormalizable because it belongs to the irreducible six-dimensional representation, $\mathbf{6}$, which appears only once in the decomposition $\mathbf{4}_1 \otimes \mathbf{4}_1 = \mathbf{1}_1 + \mathbf{3}_1 + \mathbf{3}_3 + \mathbf{3}_4 + \mathbf{6}$.

A natural question to ask is what are the equivalent representations that can really mix among themselves in the decompositions (20), (21) and (22). For a general answer see Ref. [16]. For our purposes it is enough to note here that radiative corrections can not only induce any permutation of the values of the indices, but can also make pairs of equal indices flip their common value. As an example, from O_{112} radiative corrections may generate O_{211} , O_{442} , O_{323} and the like, but not O_{123} nor O_{114} . Similarly O_{111} can mix with O_{133} , O_{414} and so on. But from O_{123} only O_{213} and permutations can arise, and not operators like O_{122} or O_{441} .

For the case of the operator (18) we thus expect mixing only among the three eight-dimensional representations that can be constructed by suitably arranging the operator components that have two and only two equal indices⁷. To deal with the mixing of these three copies of the eight-dimensional representation it is more convenient to consider the following three eight-dimensional representations⁸:

$$\begin{aligned}
i) \quad & O_{411}^q - \frac{1}{2}(O_{422}^q + O_{433}^q), \quad O_{422}^q - \frac{1}{2}(O_{411}^q + O_{433}^q), \quad \dots \\
& O_{311}^q - \frac{1}{2}(O_{322}^q + O_{344}^q), \quad O_{322}^q - \frac{1}{2}(O_{311}^q + O_{344}^q), \quad \dots \\
& \vdots \\
ii) \quad & O_{141}^q - \frac{1}{2}(O_{242}^q + O_{343}^q), \quad \dots \\
& \vdots \\
iii) \quad & O_{114}^q - \frac{1}{2}(O_{224}^q + O_{334}^q), \quad \dots \\
& \vdots
\end{aligned} \tag{23}$$

where neither symmetrization nor antisymmetrization of the indices is to be understood. The point here is that the operator (18), which is the symmetric combination of the three kinds of operators in Eqs. (23), actually mixes with the two other independent linear combinations of them that do not possess any special symmetry. In other words, the interaction may change the symmetry properties of these operators.

In the continuum the transformation properties for the rank three operators are much simpler. In fact, the symmetric combination (18) belongs to the

⁷ No mixing can occur with the operator $O_{\{41\}}^q$, because as we said it belongs to the representation **6**, which does not appear in the decomposition (20).

⁸ Apparently the number of components of each multiplet is 12 instead of 8. But in fact there are 4 constraints, because the sum of the four components of each line in (23) is zero.

sixteen-dimensional $(\frac{3}{2}, \frac{3}{2})$ irreducible representation of $O(4)$, which only appears once in the decomposition (19), and consequently the operator (18) is multiplicatively renormalizable. It follows that in the continuum, unlike what happens on the lattice, the two four-component multiplets of operators $(O_{\{111\}}^q, O_{\{222\}}^q, \dots)$ and $(O_{\{123\}}^q, O_{\{234\}}^q, \dots)$, which are part of this representation, have the same renormalization constants as the operator (18). We report in Table 5 the value of this common renormalization constant in the \overline{MS} scheme. Vice versa no mixing occurs between the operator (18) and the two other multiplets of operators with which it mixes on the lattice, because they can be arranged in the two irreducible $O(4)$ representations $(\frac{1}{2}, \frac{3}{2})$ and $(\frac{3}{2}, \frac{1}{2})$.

As for the operator $O_{\{123\}}$, on the lattice it belongs to the $\mathbf{4}_2$ representation. This representation appears only once in the product $\mathbf{4}_1 \otimes \mathbf{4}_1 \otimes \mathbf{4}_1$, implying that the operator $O_{\{123\}}$ is multiplicatively renormalizable.

In this work we have computed the renormalization constant of $O_{\{123\}}$ and the full mixing matrix of the operators (23). We have also verified that, as expected, on the lattice the traceless operator $O_{\{111\}}$ is not multiplicatively renormalizable, and that it indeed mixes with the three operators belonging to the $\mathbf{4}_1$ representations with two equal indices, as indicated in the second row of Table 2.

2.5 *On the feasibility of higher moments computations*

We conclude this section with a few observations on the operators of rank four and five.

In the case of the rank four operators, we see from Table 3 that there are two operators that are multiplicatively renormalizable. As in the rank three case, they have all indices different. One of these representations is the totally symmetric $\mathbf{1}_1$ representation, and the other is the completely antisymmetric $\mathbf{1}_2$ representation. The $\mathbf{1}_2$ representation is unique in the decomposition (21), while the $\mathbf{1}_1$ appears five times, grouped in three different patterns. But even in this case no mixing can occur, because if one starts with the pattern of indices 1234, radiative corrections can never lead to the other two kinds of patterns which the other four $\mathbf{1}_1$ representations possess, namely 1122 and 1111. For any other choice of indices mixing will be unavoidable, because all the other representations are present more than once in the decomposition (21), and at the same time they have patterns of indices that can be turned one into the other by the interaction.

The use of the rank four operator with all indices different in Monte Carlo simulations would require three components of the momentum of the hadron to be different from zero, and different among themselves.

For the rank five operators, the situation is of course even worse. In fact there are no representations that are present only once in the decomposition (22). Furthermore, we see from Table 4 that within a single pattern of indices (i.e. within a single row) a representation is never present only once, except for 11111, which is a $\mathbf{4}_1$. In this case, however, radiative corrections can induce it to mix with the ten $\mathbf{4}_1$ representations with index pattern 11222 and with the fifteen $\mathbf{4}_1$ representations with index pattern 11223. Therefore for rank five operators mixing is unavoidable.

3 Renormalization conditions

In the tree approximation the amputated non-vanishing matrix elements of the operators $O_{\mu\nu\tau}^q$ that we consider in this work are given by

$$\begin{aligned} \langle p|O_{\{123\}}^q(a)|p\rangle\Big|_{\text{amp}}^{\text{tree}} &= -\frac{1}{2}\gamma_{\{1p_2p_3\}} \quad (24) \\ \langle p|O_{411}^q - \frac{1}{2}(O_{422}^q + O_{433}^q)(a)|p\rangle\Big|_{\text{amp}}^{\text{tree}} &= -\frac{1}{2}\left(\gamma_4p_1^2 - \frac{1}{2}(\gamma_4p_2^2 + \gamma_4p_3^2)\right) \\ \langle p|O_{141}^q - \frac{1}{2}(O_{242}^q + O_{343}^q)(a)|p\rangle\Big|_{\text{amp}}^{\text{tree}} &= -\frac{1}{2}\left(\gamma_1p_1p_4 - \frac{1}{2}(\gamma_2p_2p_4 + \gamma_3p_3p_4)\right) \\ \langle p|O_{114}^q - \frac{1}{2}(O_{224}^q + O_{334}^q)(a)|p\rangle\Big|_{\text{amp}}^{\text{tree}} &= -\frac{1}{2}\left(\gamma_1p_1p_4 - \frac{1}{2}(\gamma_2p_2p_4 + \gamma_3p_3p_4)\right). \end{aligned}$$

The renormalization conditions that connect the bare operators on the lattice to the finite operators renormalized at a scale μ must be the same as the ones imposed in the continuum. We define finite renormalized operators by requiring their two quark amputated matrix elements computed at $p^2 = \mu^2$ to be equal to the corresponding tree level amplitudes. The renormalization constant $Z_{\{123\}}$ for the multiplicatively renormalizable operator $O_{\{123\}}^q$ is thus fixed in perturbation theory by simply imposing the renormalization condition:

$$\langle p|\widehat{O}_{\{123\}}^q(\mu)|p\rangle\Big|_{p^2=\mu^2} = \langle p|O_{\{123\}}^q(a)|p\rangle\Big|_{p^2=\mu^2}^{\text{tree}}, \quad (25)$$

where $Z_{\{123\}}$ is given by

$$\widehat{O}_{\{123\}}^q(\mu) = Z_{\{123\}}(\mu a)O_{\{123\}}^q(a). \quad (26)$$

The anomalous dimension of the multiplicatively renormalizable operator $O_{\{123\}}^q$ is $25/3$. For $\mu a \ll 1$, the renormalization constant of $O_{\{123\}}^q$ can be written in

the form

$$Z_{\{123\}}(\mu a) = 1 - \frac{\alpha_S}{4\pi} C_F \left(\frac{25}{3} \log \mu a + B_{\{123\}} \right), \quad (27)$$

where $\alpha_S = g_0^2/4\pi$ and $C_F = (N_c^2 - 1)/2N_c$ is the quadratic Casimir of the fundamental representation of $SU(N_c)$; in QCD $N_c = 3$ and $C_F = 4/3$. The constant $B_{\{123\}}$ is all we have to know to fix $Z_{\{123\}}$ and is given in Sect. 5 for different values of the Wilson parameter r .

For the case in which two of the indices are equal, we see that two of the three possible combinations give the same tree level result (see Eqs. (24)). Therefore we can reduce the whole problem of mixing to the mixing of the two operators

$$O_A \equiv O_{411}^q - \frac{1}{2}(O_{422}^q + O_{433}^q) \quad (28)$$

and

$$O_B \equiv O_{141}^q + O_{114}^q - \frac{1}{2}(O_{242}^q + O_{224}^q + O_{343}^q + O_{334}^q). \quad (29)$$

If we set

$$\begin{aligned} \hat{O}_A &= Z_{AA} O_A + Z_{AB} O_B \\ \hat{O}_B &= Z_{BA} O_A + Z_{BB} O_B, \end{aligned} \quad (30)$$

the mixing coefficients will be extracted from the 1-loop calculations according to the formulae

$$\begin{aligned} \langle p|O_A|p \rangle \Big|_{p^2=\mu^2}^{1\text{-loop}} &= -\frac{1}{2} \left(Z_{AA}^{-1} \left(\gamma_4 p_1^2 - \frac{1}{2}(\gamma_4 p_2^2 + \gamma_4 p_3^2) \right) \right. \\ &\quad \left. + 2Z_{AB}^{-1} \left(\gamma_1 p_1 p_4 - \frac{1}{2}(\gamma_2 p_2 p_4 + \gamma_3 p_3 p_4) \right) \right) \\ \langle p|O_B|p \rangle \Big|_{p^2=\mu^2}^{1\text{-loop}} &= -\frac{1}{2} \left(Z_{BA}^{-1} \left(\gamma_4 p_1^2 - \frac{1}{2}(\gamma_4 p_2^2 + \gamma_4 p_3^2) \right) \right. \\ &\quad \left. + 2Z_{BB}^{-1} \left(\gamma_1 p_1 p_4 - \frac{1}{2}(\gamma_2 p_2 p_4 + \gamma_3 p_3 p_4) \right) \right). \end{aligned} \quad (31)$$

Taking into account the form of the matrix of the anomalous dimensions of O_A and O_B (see Table 11), we can write

$$Z_{AA}(\mu a) = 1 - \frac{\alpha_S}{4\pi} C_F \left(\frac{13}{3} \log \mu a + B_{AA} \right)$$

$$\begin{aligned}
Z_{AB}(\mu a) &= -\frac{\alpha_S}{4\pi} C_F (2 \log \mu a + B_{AB}) \\
Z_{BA}(\mu a) &= -\frac{\alpha_S}{4\pi} C_F (4 \log \mu a + B_{BA}) \\
Z_{BB}(\mu a) &= 1 - \frac{\alpha_S}{4\pi} C_F \left(\frac{19}{3} \log \mu a + B_{BB} \right), \tag{32}
\end{aligned}$$

where the values of the constants B can be found in Sect. 5.

For DIS the physically relevant operator is the symmetric combination O_{DIS}^q (Eq. (18)), which is simply given by

$$O_{\text{DIS}}^q = \frac{1}{3} (O_A + O_B). \tag{33}$$

For it we have

$$\begin{aligned}
\widehat{O}_{\text{DIS}}^q(\mu) &= \frac{1}{3} (\widehat{O}_A(\mu) + \widehat{O}_B(\mu)) \\
&= \frac{1}{3} (Z_{AA} + Z_{BA}) O_A + \frac{1}{3} (Z_{AB} + Z_{BB}) O_B. \tag{34}
\end{aligned}$$

4 Some aspects of the computation

The computation of the renormalization constant of the operator $O_{\{123\}}$ has been crosschecked by comparing the results obtained from two completely independent codes, written to automatically carry out all the extremely complicated algebraic manipulations necessary in the calculation [17]. In fact, contrary to the case of the rank two operator, no complete hand checks are possible here⁹: the operator of rank three contains one more covariant derivative, and all propagators, vertices and operators have to be expanded to second order in a . This results in impossibly long algebraic expressions. In the case of the operator with two equal indices we have checked by hand the results only for the simplest Feynman diagrams.

We started our computations by employing a Schoonschip code [18] which was obtained as an evolution of the one we used in Ref. [1]. At a later stage we decided to use the more flexible Form language, and we developed a completely new set of routines to deal with Dirac γ -matrices.

⁹ We have completed the calculations by hand only for the non-improved diagrams; the calculations of the improved ones is hard drudgery.

The most innovative feature of the new Form program is a routine that reduces the products of γ -matrices in a much more efficient way than before. As a byproduct, the treatment of even products of sines¹⁰ can be postponed, and performed after the completion of the Dirac algebra; in this way, we happily no longer need to evaluate the daring expressions involving six and eight sines that gave rise to a plethora of terms (see Tables C.2 and C.3 in Ref. [1]) in the old Schoonschip programs. One discovers that what is needed in this new way of proceeding is at most the peculiar combination of six sines of the kind

$$\begin{aligned}
\mathcal{I}(\mu_1, \mu_2, \mu_3, \mu_4) &= \int d^4k f(\cos k, \sum_{\lambda} \sin^2 k_{\lambda}) \sin k_{\mu_1} \sin k_{\mu_2} \sin k_{\mu_3} \sin^3 k_{\mu_4} = \\
&\int d^4k f(\cos k, \sum_{\lambda} \sin^2 k_{\lambda}) \sin^2 k_{\mu_1} \sin^4 k_{\mu_3} \delta_{\mu_1\mu_2} \delta_{\mu_3\mu_4} \\
&+ \int d^4k f(\cos k, \sum_{\lambda} \sin^2 k_{\lambda}) \sin^2 k_{\mu_1} \sin^4 k_{\mu_2} \delta_{\mu_1\mu_3} \delta_{\mu_2\mu_4} \\
&+ \int d^4k f(\cos k, \sum_{\lambda} \sin^2 k_{\lambda}) \sin^4 k_{\mu_1} \sin^2 k_{\mu_2} \delta_{\mu_1\mu_4} \delta_{\mu_2\mu_3} \\
&- 2 \cdot \int d^4k f(\cos k, \sum_{\lambda} \sin^2 k_{\lambda}) \sin^6 k_{\mu_1} \delta_{\mu_1\mu_2\mu_3\mu_4}, \tag{35}
\end{aligned}$$

where $\delta_{\mu_1\mu_2\mu_3\mu_4}$ is non-zero only if all the indices are equal. The structure and the coefficients of Eq. (35) are the same as those that appear in the similar formula for the case of four sines (see Table C.1 in Ref. [1]), with a sine raised to the third power here playing the role of a plain sine there.

The Form code described above is the one that has been carefully optimized and used more extensively in our computations. Meanwhile, another Form code, completely independent from it, has been developed by one of us [19]. Summarizing, three sets of routines have grown up from our efforts, and we have checked for each code separately that the rather complicated Dirac algebra (we have products of up to seven gamma matrices) is carried out correctly. The analytical results obtained with the modified old Schoonschip program and with the two newly developed Form codes have been compared, and they turn out to be in perfect agreement. This we regard as a significative check of our calculations.

The numerical integration has also been performed using various different Fortran programs, that all gave the same results within a 1% relative error. For the numerical integration, and for the treatment of the logarithmic divergences, we have used the same strategy as in Ref. [1] and once more we refer the reader to that paper for details.

¹⁰ Odd number of sines integrates to zero.

A big problem we have encountered was the limitation on the working memory allowed by Schoonschip and Form on the different machines we have used. This is of primary relevance in the first stages of the computation, when all vertices, propagators etc. have to be expanded up to second order in the lattice spacing a . When dealing with the rank three case, one encounters several products of up to ten trigonometric functions, each one to be expanded up to order a^2 . Every product at first will thus give rise to something like 10^4 monomials. A large part of them does not contribute to the final expression, to the order in a we are interested in, and has to be killed at the earliest possible stage of the calculation. A careless way of programming may lead to an increase of CPU times of several orders of magnitude, or even to an abrupt stop of the elaboration for lack of memory.

In going to the new Form programs, and thanks to the evolution of the various routines, the CPU time needed to perform the whole analytic calculation was drastically cut down. The CPU time required by the old Schoonschip code running on a Sun 3 workstation ranged from a few minutes up to more than four hours for the most complicated diagrams. The Form program was first running on VAX-VMS machines and then on a HP-UX 9000/735 machine. In its present form the computation of a generic diagram only takes from about ten seconds up to a few minutes.

We conclude this section with a discussion on an important physical point that needs some clarification. This is the role of the terms $a^2 p^2$ that appear in what we may call the effective ‘‘Feynman propagator’’, $P(ak, ap; q)$, of a diagram, i.e. the overall denominator that arises after the introduction of the Feynman parameters. Generally it will have the form

$$P(ak, ap; q) = \left[g(ak) + ap_\mu h_\mu(ak) + \alpha(1 - \alpha)a^2 p^2 + a^2 p_\mu p_\nu f_{\mu\nu}(ak) \right]^q, \quad (36)$$

with $q \geq 2$, where the functions $h_\mu(ak)$ and $f_{\mu\nu}(ak)$ have the following small ak behavior:

$$\begin{aligned} h_\mu(ak) &\stackrel{ak \rightarrow 0}{\sim} (ak)^3 \\ f_{\mu\nu}(ak) &\stackrel{ak \rightarrow 0}{\sim} (ak)^2. \end{aligned} \quad (37)$$

We see that the terms $a^2 p^2$ enter either multiplied by a function of ak vanishing as $ak \rightarrow 0$ (e.g. $\sin^2 ak$, $1 - \cos ak$ etc.) or by a constant independent of a (i.e. $\alpha(1 - \alpha)a^2 p^2$). They should be treated differently according to whether the diagram has already the required $p_\mu p_\nu$ tensor structure in front or whether this structure will emerge after expanding the Feynman denominator itself. For dimensional reasons in the first case the diagram will be logarithmically divergent. Terms such as $ap_\mu h_\mu(ak)$ and $a^2 p_\mu p_\nu f_{\mu\nu}(ak)$ are to be set to zero,

Table 5

Values of the constant $B_{(\frac{3}{2}, \frac{3}{2})}$ in the \overline{MS} regularization scheme

	sails	-62/9
$B_{(\frac{3}{2}, \frac{3}{2})}^{\overline{MS}}$	vertex	4/9
	self-energy	-1
	total	-67/9

while the term $\alpha(1 - \alpha)a^2p^2$ must be kept in the denominator and will act as a regulator for the lattice infrared singularity at $ak = 0$. In the limit $ap \ll 1$ it will give rise to the expected logarithmic behavior, $\log ap$. In the second case the integral is finite because a function of ak , vanishing as $(ak)^2$ in the limit $ak \rightarrow 0$, will dimensionally replace in the numerator the two missing momenta present in the previous case. In this situation the contribution of the diagram to the sought tensor structure is obtained by expanding the Feynman propagator in powers of $a^2p_\mu p_\nu f_{\mu\nu}(ak)$. Each term in this expansion is finite, thanks to the smoothing out provided by the function $f_{\mu\nu}(ak)$, and one is allowed to set to zero the $\alpha(1 - \alpha)a^2p^2$ term. Since we are interested in the terms that have at most two powers of p in front, we must look in the expansion only to the terms that are linear in $a^2p_\mu p_\nu f_{\mu\nu}(ak)$.

Similarly $P(ak, ap; q)$ must be expanded in powers of $ap_\mu h_\mu(ak)$ up to second order. Linear and quadratic terms must be kept in the expansion to combine with the possible p -dependence present in the numerator and reconstruct the required $p_\mu p_\nu$ tensor structure. The coefficients of this expansion are finite loop momentum integrals in which all a^2p^2 terms can be safely set to zero.

5 Results

The results of our calculations are summarized in the Tables 5–12 presented in this section. The contributions coming from the standard Wilson action (that is, the non-improved results), those coming from the terms naively of order a in the improvement procedure and those coming from the terms naively of order a^2 are shown separately. Contributions from different classes of diagrams, according to the classification given in Appendix B, are also presented separately. The accuracy of the numbers presented here depends only on the accuracy of the numerical integration and it is better than 1%.

In Table 5 we give the continuum \overline{MS} renormalization constants of the operators $O_{\{123\}}$, $O_A + O_B$ and $O_{\{111\}}$. In Table 6 the results for the lattice renormalization constants of the multiplicatively renormalizable operator $O_{\{123\}}$ are reported. Our numbers for the Wilson case agree, within errors, with

Table 6
Values of $B_{\{123\}}$

	r	Wilson	$O(a)$ impr.	$O(a^2)$ impr.	total
SAILS	0.2	-4.172	-1.611	-0.022	-5.805
	0.4	-5.368	-3.683	-0.106	-9.157
	0.6	-6.309	-5.033	-0.271	-11.612
	0.8	-7.032	-5.838	-0.520	-13.389
	1.0	-7.607	-6.313	-0.854	-14.773
VERTEX	0.2	0.387	-0.060	0.012	0.339
	0.4	0.574	-0.215	0.064	0.423
	0.6	0.804	-0.398	0.162	0.568
	0.8	1.021	-0.572	0.307	0.756
	1.0	1.216	-0.731	0.500	0.984
$\frac{1}{2}$ SELF-ENERGY	0.2	-6.102	-0.611	0	-6.713
	0.4	-4.326	-1.513	0	-5.839
	0.6	-2.762	-2.311	0	-5.073
	0.8	-1.465	-3.013	0	-4.479
	1.0	-0.381	-3.646	0	-4.027
operator TADPOLE + $\frac{1}{2}$ leg TADPOLE	0.2	-12.233	0	0.009	-12.224
	0.4	-12.233	0	0.037	-12.196
	0.6	-12.233	0	0.084	-12.149
	0.8	-12.233	0	0.150	-12.083
	1.0	-12.233	0	0.234	-11.999
TOTAL	0.2	-22.121	-2.282	-0.000	-24.403
	0.4	-21.353	-5.411	-0.005	-26.769
	0.6	-20.500	-7.741	-0.025	-28.266
	0.8	-19.709	-9.424	-0.063	-29.195
	1.0	-19.005	-10.690	-0.120	-29.815

those of Ref. [20]. In Tables 7–10 we give, for $r = 1$ only, the values of the four lattice B constants relevant for the mixing between the operators $O_A = O_{411}^q - \frac{1}{2}(O_{422}^q + O_{433}^q)$ and $O_B = O_{141}^q + O_{114}^q - \frac{1}{2}(O_{242}^q + O_{224}^q + O_{343}^q + O_{334}^q)$. In Table 11 for completeness we report the mixing matrix of the anomalous dimensions of these operators. In Table 12 a summary of the mixing matrices

Table 7

Values of B_{AA} for $r = 1$

	Wilson	$O(a)$ impr.	$O(a^2)$ impr.	total
SAILS	-2.353	-3.568	-5.582	-11.502
VERTEX	0.870	-0.258	0.384	0.996
$\frac{1}{2}$ SELF-ENERGY	-0.381	-3.646	0	-4.027
operator TADPOLE				
+	-16.960	0	4.104	-12.856
$\frac{1}{2}$ leg TADPOLE				
TOTAL	-18.824	-7.472	-1.093	-27.389

Table 8

Values of B_{AB} for $r = 1$

	Wilson	$O(a)$ impr.	$O(a^2)$ impr.	total
SAILS	-0.953	-1.183	2.391	0.255
VERTEX	0.029	-0.245	0.007	-0.208
$\frac{1}{2}$ SELF-ENERGY	0	0	0	0
operator TADPOLE				
+	0	0	-3.649	-3.649
$\frac{1}{2}$ leg TADPOLE				
TOTAL	-0.924	-1.428	-1.251	-3.603

Table 9

Values of B_{BA} for $r = 1$

	Wilson	$O(a)$ impr.	$O(a^2)$ impr.	total
SAILS	-3.108	-4.731	5.465	-2.373
VERTEX	0.153	-0.556	-0.044	-0.448
$\frac{1}{2}$ SELF-ENERGY	0	0	0	0
operator TADPOLE				
+	0	0	-8.982	-8.982
$\frac{1}{2}$ leg TADPOLE				
TOTAL	-2.955	-5.287	-3.562	-11.803

Table 10
 Values of B_{BB} for $r = 1$

	Wilson	$O(a)$ impr.	$O(a^2)$ impr.	total
SAILS	-6.421	-3.899	-4.313	-14.633
VERTEX	1.494	-0.462	0.725	1.758
$\frac{1}{2}$ SELF-ENERGY	-0.381	-3.646	0	-4.027
operator TADPOLE				
+	-12.233	0	10.596	-1.637
$\frac{1}{2}$ leg TADPOLE				
TOTAL	-17.540	-8.006	7.009	-18.538

Table 11
 Mixing matrix of the anomalous dimensions of the operators O_A and O_B

ANOMALOUS DIMENSIONS	
SAILS	$\begin{bmatrix} 10/3 & 5/3 \\ 10/3 & 5 \end{bmatrix}$
VERTEX	$\begin{bmatrix} -1 & 1/3 \\ 2/3 & -2/3 \end{bmatrix}$
$\frac{1}{2}$ SELF-ENERGY	$\begin{bmatrix} 2 & 0 \\ 0 & 2 \end{bmatrix}$
TOTAL	$\begin{bmatrix} 13/3 & 2 \\ 4 & 19/3 \end{bmatrix}$

for the B constants both in continuum \overline{MS} and on the lattice (where we give separately the results for the Wilson case and for the fully improved case) is given.

Two observations are in order here. First of all we notice that for the physically relevant symmetric operator $O_{\text{DIS}}^g = \frac{1}{3}(O_A + O_B)$ the sum of the elements in each column of the lattice matrices are not equal, signalling that mixing

Table 12

Mixing matrix for the B constants (the lattice values are for $r = 1$)

	Continuum \overline{MS}	Lattice (Wilson)	Lattice (full improved)
SAILS	$\begin{pmatrix} -\frac{31}{9} & -\frac{31}{18} \\ -\frac{31}{9} & -\frac{93}{18} \end{pmatrix}$	$\begin{pmatrix} -2.353 & -0.953 \\ -3.108 & -6.421 \end{pmatrix}$	$\begin{pmatrix} -11.502 & 0.255 \\ -2.373 & -14.633 \end{pmatrix}$
VERTEX	$\begin{pmatrix} \frac{8}{9} & \frac{1}{9} \\ \frac{2}{9} & 1 \end{pmatrix}$	$\begin{pmatrix} 0.870 & 0.029 \\ 0.153 & 1.494 \end{pmatrix}$	$\begin{pmatrix} 0.996 & -0.208 \\ -0.448 & 1.758 \end{pmatrix}$
$\frac{1}{2}$ SELF-ENERGY	$\begin{pmatrix} -1 & 0 \\ 0 & -1 \end{pmatrix}$	$\begin{pmatrix} -0.381 & 0 \\ 0 & -0.381 \end{pmatrix}$	$\begin{pmatrix} -4.027 & 0 \\ 0 & -4.027 \end{pmatrix}$
TADPOLES		$\begin{pmatrix} -16.960 & 0 \\ 0 & -12.233 \end{pmatrix}$	$\begin{pmatrix} -12.856 & -3.649 \\ -8.982 & -1.637 \end{pmatrix}$
TOTAL	$\begin{pmatrix} -\frac{32}{9} & -\frac{29}{18} \\ -\frac{29}{9} & -\frac{93}{18} \end{pmatrix}$	$\begin{pmatrix} -18.824 & -0.924 \\ -2.955 & -17.540 \end{pmatrix}$	$\begin{pmatrix} -27.389 & -3.603 \\ -11.803 & -18.538 \end{pmatrix}$

occurs. In the continuum instead, as expected from the discussion of Sect. 2, it can be easily checked from the numbers given in Tables 11 and 12 that the combination $O_A + O_B$ is in fact multiplicatively renormalizable. A second observation that emerges by looking at the results of Table 12 is that, at least in this case, one should talk of “tadpole + sails dominance” rather than simply of “tadpole dominance” in lattice perturbation theory.

We may summarize the results obtained in this paper in the following formulae.

1) Standard Wilson action (Tables 6 and 12):

$$\begin{aligned}
\widehat{O}_{\{123\}}^q &= \left[1 - \frac{25}{6\pi^2\beta} \log \mu a - \frac{1}{2\pi^2\beta} B_{\{123\}} \right] O_{\{123\}}^q \\
&= \left[1 - \frac{0.422}{\beta} \log \mu a + \frac{0.963}{\beta} \right] O_{\{123\}}^q, \tag{38}
\end{aligned}$$

$$\begin{aligned}
\widehat{O}_{\text{DIS}}^q &= \frac{1}{3} \left[1 - \frac{25}{6\pi^2\beta} \log \mu a - \frac{1}{2\pi^2\beta} (B_{AA} + B_{BA}) \right] O_A \\
&\quad + \frac{1}{3} \left[1 - \frac{25}{6\pi^2\beta} \log \mu a - \frac{1}{2\pi^2\beta} (B_{AB} + B_{BB}) \right] O_B \\
&= \frac{1}{3} \left[1 - \frac{0.422}{\beta} \log \mu a + \frac{1.103}{\beta} \right] O_A + \frac{1}{3} \left[1 - \frac{0.422}{\beta} \log \mu a + \frac{0.935}{\beta} \right] O_B. \quad (39)
\end{aligned}$$

2) Nearest-neighbor improved action (Tables 6 and 12)

$$\begin{aligned}
(\widehat{O}_{\{123\}}^q)^{\text{I}} &= \left[1 - \frac{25}{6\pi^2\beta} \log \mu a - \frac{1}{2\pi^2\beta} B_{\{123\}}^{\text{I}} \right] (O_{\{123\}}^q)^{\text{I}} \\
&= \left[1 - \frac{0.422}{\beta} \log \mu a + \frac{1.510}{\beta} \right] (O_{\{123\}}^q)^{\text{I}}, \quad (40)
\end{aligned}$$

$$\begin{aligned}
(\widehat{O}_{\text{DIS}}^q)^{\text{I}} &= \frac{1}{3} \left[1 - \frac{25}{6\pi^2\beta} \log \mu a - \frac{1}{2\pi^2\beta} (B_{AA}^{\text{I}} + B_{BA}^{\text{I}}) \right] (O_A)^{\text{I}} \\
&\quad + \frac{1}{3} \left[1 - \frac{25}{6\pi^2\beta} \log \mu a - \frac{1}{2\pi^2\beta} (B_{AB}^{\text{I}} + B_{BB}^{\text{I}}) \right] (O_B)^{\text{I}} \\
&= \frac{1}{3} \left[1 - \frac{0.422}{\beta} \log \mu a + \frac{1.985}{\beta} \right] (O_A)^{\text{I}} \\
&\quad + \frac{1}{3} \left[1 - \frac{0.422}{\beta} \log \mu a + \frac{1.122}{\beta} \right] (O_B)^{\text{I}}. \quad (41)
\end{aligned}$$

Obviously physical quantities should at the end be independent from the chosen regularization procedure. In particular the dependence from the subtraction point, μ , must disappear from physical hadronic matrix elements. In fact, consistently to each order in perturbation theory, the $\log \mu a$ terms get canceled in the product between the Wilson coefficients and the matrix elements of the renormalized operators that are eigenvectors of the anomalous dimension matrix. The net result is that effectively the Wilson coefficients must be taken at a momentum scale a^{-1} and the operators turn out to be effectively renormalized by “reduced” renormalization constants \widetilde{Z} , obtained from the full expressions by dropping all $\log \mu a$ terms.

Numerically for $N_c = 3$ at the typical values $\beta \equiv 2N_c/g_0^2 = 6$ and $r = 1$ and in the quenched approximation, one gets for the unmixed quark operator $O_{\{123\}}^q$ from Eqs. (38) and (40)

$$\begin{aligned}\tilde{O}_{\{123\}}^q &= 1.160 O_{\{123\}}^q && \text{Wilson case} \\ (\tilde{O}_{\{123\}}^q)^I &= 1.252 (O_{\{123\}}^q)^I && \text{Improved case ,}\end{aligned}$$

where by the superscript \sim we mean that the $\log \mu a$ term has been dropped from the expression of the Z 's, as explained before.

Similarly in the case of the operator O_{DIS}^q one has from Eqs. (39) and (41)

$$\begin{aligned}\tilde{O}_{\text{DIS}}^q &= \frac{1}{3} [1.184 O_A + 1.156 O_B] && \text{Wilson case} \\ (\tilde{O}_{\text{DIS}}^q)^I &= \frac{1}{3} [1.331 (O_A)^I + 1.187 (O_B)^I] && \text{Improved case .}\end{aligned}$$

In the existing simulations corrections due to renormalization and mixing effects were either calculated by means of tadpole dominance [14,15] or for simplicity neglected [21]. We see that even this latter approximation is not quite adequate because the effective renormalization constants and mixing coefficients are not small. It should also be noted that the renormalization constants do not seem to decrease in magnitude with the order N of the moment. This fact is already evident in the Wilson case, where the renormalization constants of the rank three operators are larger than those of the rank two quark operators (see Ref. [1]), and it is confirmed by the complete improved computation.

A Perturbative expansion of the vertex operator $(O_{\mu\nu\tau}^q)^I$

In this appendix we present the perturbative expansion of the vertex operator $(O_{\mu\nu\tau}^q)^I$, given by Eq. (11). We have used the definitions

$$\overrightarrow{D}_\mu \psi_n = \frac{1}{2a} [U_{n,\nu} \psi_{n+\mu} - U_{n-\mu,\mu}^+ \psi_{n-\mu}] \quad (\text{A.1})$$

$$\overleftarrow{D}_\mu \bar{\psi} = \frac{1}{2a} [\bar{\psi}_{n+\mu} U_{n,\nu}^+ - \bar{\psi}_{n-\mu} U_{n-\mu,\mu}],$$

and the conventions

$$A_{n,\mu} = \int \frac{d^4 q}{(2\pi)^4} e^{i(q + q_\mu/2)n} A_\mu(q) \quad (\text{A.2})$$

$$\psi_n = \int \frac{d^4 q}{(2\pi)^4} e^{iqn} \psi(q) \quad (\text{A.3})$$

$$\bar{\psi}_n = \int \frac{d^4 q}{(2\pi)^4} e^{-iqn} \bar{\psi}(q), \quad (\text{A.4})$$

where the integrals are performed over the first Brillouin zone. Throughout this appendix external and loop momenta are expressed in lattice units.

Since the full Fourier transform of the operator $(O_{\mu\nu\tau}^q)^I$ is very complicated, we give here only the form it effectively takes when inserted in the diagrams of Fig. B.2. Calling p the external incoming and outgoing momentum, and k the fermion loop momentum, one finds, separating the various contributions according to their naive order in a :

a) tree level

$$\begin{aligned}
(O_{\mu\nu\tau}^q)^I(n=0)|_{tree} &= -\frac{1}{2} \int_{-\pi}^{\pi} \frac{d^4k}{(2\pi)^4} \bar{\psi}(k) \gamma_{\mu} \frac{\sin k_{\nu}}{a} \frac{\sin k_{\tau}}{a} \psi(k) \\
&+ \frac{i a r}{2} \int_{-\pi}^{\pi} \frac{d^4k}{(2\pi)^4} \bar{\psi}(k) \frac{\sin k_{\mu}}{a} \frac{\sin k_{\nu}}{a} \frac{\sin k_{\tau}}{a} \psi(k) \\
&+ \frac{a^2 r^2}{8} \int_{-\pi}^{\pi} \frac{d^4k}{(2\pi)^4} \bar{\psi}(k) \sum_{\lambda, \lambda'} \gamma_{\lambda} \gamma_{\mu} \gamma_{\lambda'} \frac{\sin k_{\lambda}}{a} \frac{\sin k_{\lambda'}}{a} \frac{\sin k_{\nu}}{a} \frac{\sin k_{\tau}}{a} \psi(k).
\end{aligned} \tag{A.5}$$

b) order g_0

$$\begin{aligned}
(O_{\mu\nu\tau}^q)^I(n=0)|_{g_0} &= -\frac{g_0}{2} \int_{-\pi}^{\pi} \frac{d^4k}{(2\pi)^4} \bar{\psi}(p) \gamma_{\mu} \left[\cos\left(\frac{k+p}{2}\right)_{\nu} \frac{\sin k_{\tau}}{a} A_{\nu}(p-k) \right. \\
&+ \left. \cos\left(\frac{k+p}{2}\right)_{\tau} \frac{\sin p_{\nu}}{a} A_{\tau}(p-k) \right] \psi(k) \\
&+ \frac{i a g_0 r}{4} \int_{-\pi}^{\pi} \frac{d^4k}{(2\pi)^4} \bar{\psi}(p) \sum_{\lambda} \left\{ \gamma_{\mu} \gamma_{\lambda} \left[\cos\left(\frac{k+p}{2}\right)_{\nu} \frac{\sin k_{\tau}}{a} \frac{\sin k_{\lambda}}{a} A_{\nu}(p-k) \right. \right. \\
&+ \cos\left(\frac{k+p}{2}\right)_{\tau} \frac{\sin k_{\lambda}}{a} \frac{\sin p_{\nu}}{a} A_{\tau}(p-k) \\
&+ \left. \left. \cos\left(\frac{k+p}{2}\right)_{\lambda} \frac{\sin p_{\nu}}{a} \frac{\sin p_{\tau}}{a} A_{\lambda}(p-k) \right] \right. \\
&+ \left. \gamma_{\lambda} \gamma_{\mu} \left[\cos\left(\frac{k+p}{2}\right)_{\nu} \frac{\sin k_{\tau}}{a} \frac{\sin p_{\lambda}}{a} A_{\nu}(p-k) \right. \right. \\
&+ \cos\left(\frac{k+p}{2}\right)_{\tau} \frac{\sin p_{\nu}}{a} \frac{\sin p_{\lambda}}{a} A_{\tau}(p-k) \\
&+ \left. \left. \cos\left(\frac{k+p}{2}\right)_{\lambda} \frac{\sin k_{\nu}}{a} \frac{\sin k_{\tau}}{a} A_{\lambda}(p-k) \right] \right\} \psi(k)
\end{aligned} \tag{A.6}$$

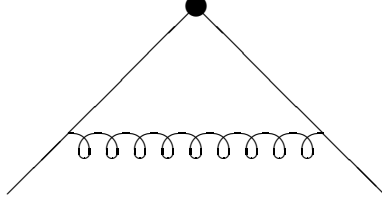


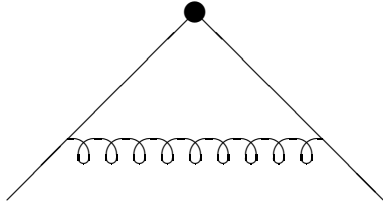
Fig. B.1. The graph that symbolically represents the 1-loop vertex correction to the insertion of the $(O_{\mu\nu}^q)^1$ operator. The operator insertion is indicated by a dot. The wavy line is a gluon.

$$\begin{aligned}
& + \frac{a^2 g_0 r^2}{8} \int_{-\pi}^{\pi} \frac{d^4 k}{(2\pi)^4} \bar{\psi}(p) \sum_{\lambda, \lambda'} \gamma_{\lambda} \gamma_{\mu} \gamma_{\lambda'} \left[\cos\left(\frac{k+p}{2}\right)_{\nu} \frac{\sin p_{\lambda'}}{a} \frac{\sin k_{\tau}}{a} \frac{\sin k_{\lambda}}{a} A_{\nu}(p-k) \right. \\
& \quad + \cos\left(\frac{k+p}{2}\right)_{\tau} \frac{\sin p_{\nu}}{a} \frac{\sin p_{\lambda'}}{a} \frac{\sin k_{\lambda}}{a} A_{\tau}(p-k) \\
& \quad + \cos\left(\frac{k+p}{2}\right)_{\lambda} \frac{\sin k_{\nu}}{a} \frac{\sin k_{\tau}}{a} \frac{\sin k_{\lambda'}}{a} A_{\lambda}(p-k) \\
& \quad \left. + \cos\left(\frac{k+p}{2}\right)_{\lambda'} \frac{\sin p_{\nu}}{a} \frac{\sin p_{\tau}}{a} \frac{\sin p_{\lambda'}}{a} A_{\lambda'}(p-k) \right] \psi(k).
\end{aligned}$$

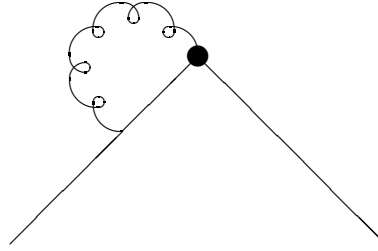
The above formula is given in the kinematical configuration in which the incoming gluon momentum lands on the incoming quark leg. If the gluon is attached to the outgoing quark leg, one must exchange p and k . Notice that the first lines in Eqs. (A.5) and (A.6) correspond to the non-improved expression of the operator.

We do not give here the expression of the $O(g_0^2)$ terms because, besides being extremely complicated, they are not actually necessary for our computation. In fact we need them only when either the gluon or the quark legs are contracted to make a tadpole loop, and in this situation the tadpole directly factorizes out.

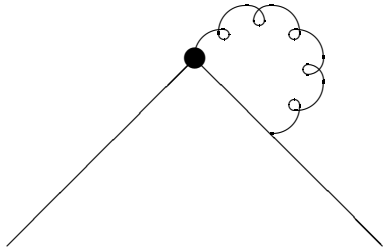
The case in which two or more indices are identical is easily derived from the expressions above.



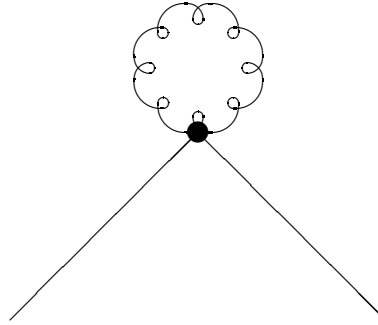
(a) Vertex



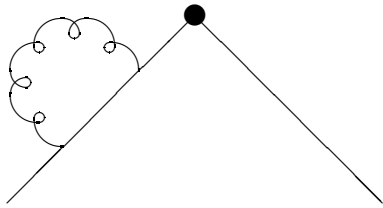
(b) Sail



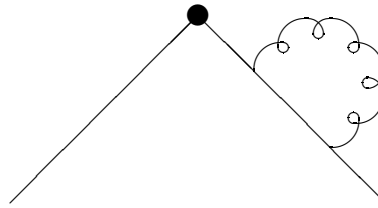
(c) Sail



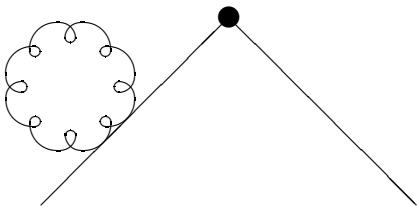
(d) Operator tadpole



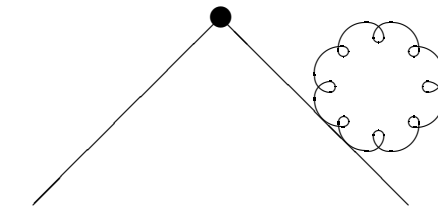
(e) Self-energy



(f) Self-energy



(g) Leg tadpole



(h) Leg tadpole

Fig. B.2. The different types of graphs contributing to the 1-loop approximation of the matrix element $\langle p | (O_{\mu\nu\tau}^q)^I | p \rangle$.

B Diagrams

In what follows we show the 1-loop diagrams that we have calculated for each one of the operators discussed in this work. They are accompanied by a label that allows an easy connection with the Tables presented in Sect. 5.

Actually, each graph in this appendix corresponds to several diagrams in the perturbative expansion. For example, the vertex correction of Fig. B.1 symbolically represents the sum of 12 different diagrams. They come out remembering that for the quark-gluon interaction one can either take the standard Wilson vertex of Eq. (7) or the improved vertex of Eq. (8), and for the operator insertion either its unrotated form or the $O(a)$ or else the $O(a^2)$ corrections (see Eqs. (11) and (A.5)).

We report in Fig. B.2 the types of graphs that contribute to the 1-loop calculation of the matrix element $\langle p|(O_{\mu\nu\tau}^q)^I|p\rangle$, with the understanding that the drawings we show are representative of the structure of full sets of improved diagrams.

C α -integration

To reduce the computing time in the numerical evaluation of the integrals that involve fermion propagators, we have chosen to perform analytically the integration over the Feynman parameter α , and to leave for the numerical integration only a four-dimensional expression. To this end after the subtraction of the standard logarithmic divergence we need to compute integrals of the form

$$F_{nm}(f(k), g(k)) = \int_0^1 d\alpha \frac{\alpha^n}{[f(k) + \alpha g(k)]^m}. \quad (\text{C.1})$$

In our calculations we explicitly have

$$\begin{aligned} g(k) &= 4 \sum_{\lambda} \sin^2 \frac{k_{\lambda}}{2} - \left[\sum_{\lambda} \sin^2 k_{\lambda} + 4r^2 \left(\sum_{\lambda} \sin^2 \frac{k_{\lambda}}{2} \right)^2 \right] \\ f(k) &= \left[\sum_{\lambda} \sin^2 k_{\lambda} + 4r^2 \left(\sum_{\lambda} \sin^2 \frac{k_{\lambda}}{2} \right)^2 \right]. \end{aligned} \quad (\text{C.2})$$

The functions F_{nm} satisfy the recurrence relations

$$\frac{\partial}{\partial f} F_{nm} = -m \cdot F_{n \ m+1} \quad (\text{C.3})$$

$$\frac{\partial}{\partial g} F_{nm} = -m \cdot F_{n+1 \ m+1} \quad (\text{C.4})$$

which make simpler their computation and allow for a check of the formulae given below.

The formulae needed in this work are:

$$\begin{aligned} F_{02} &= \frac{1}{f \cdot (g+f)} \\ F_{12} &= \frac{1}{g} \cdot \left[\frac{1}{g} \log \left(1 + \frac{g}{f} \right) - \frac{1}{g+f} \right] \\ F_{22} &= \frac{1}{g^2} \cdot \left[1 - 2 \frac{f}{g} \log \left(1 + \frac{g}{f} \right) + \frac{f}{g+f} \right] \\ F_{32} &= \frac{1}{g^2} \cdot \left[\frac{1}{2} - 2 \frac{f}{g} + 3 \frac{f^2}{g^2} \log \left(1 + \frac{g}{f} \right) - \frac{f^2}{g \cdot (g+f)} \right] \\ F_{42} &= \frac{1}{g^2} \cdot \left[\frac{1}{3} - \frac{f}{g} + 3 \frac{f^2}{g^2} - 4 \frac{f^3}{g^3} \log \left(1 + \frac{g}{f} \right) + \frac{f^3}{g^2 \cdot (g+f)} \right] \\ F_{03} &= \frac{g+2f}{2f^2 \cdot (g+f)^2} \\ F_{13} &= \frac{1}{2f \cdot (g+f)^2} \\ F_{23} &= \frac{1}{g^2} \cdot \left[\frac{1}{g} \log \left(1 + \frac{g}{f} \right) - \frac{3g+2f}{2 \cdot (g+f)^2} \right] \\ F_{33} &= \frac{1}{g^3} \cdot \left[1 - 3 \frac{f}{g} \log \left(1 + \frac{g}{f} \right) + f \frac{5g+4f}{2 \cdot (g+f)^2} \right] \\ F_{43} &= \frac{1}{g^3} \cdot \left[\frac{1}{2} - 3 \frac{f}{g} + 6 \frac{f^2}{g^2} \log \left(1 + \frac{g}{f} \right) - f^2 \frac{7g+6f}{2g \cdot (g+f)^2} \right] \\ F_{53} &= \frac{1}{g^3} \cdot \left[\frac{1}{3} - \frac{3f}{2g} + 6 \frac{f^2}{g^2} - 10 \frac{f^3}{g^3} \log \left(1 + \frac{g}{f} \right) + f^3 \frac{9g+8f}{2g^2 \cdot (g+f)^2} \right] \\ F_{63} &= \frac{1}{g^3} \cdot \left[\frac{1}{4} - \frac{f}{g} + 3 \frac{f^2}{g^2} - 10 \frac{f^3}{g^3} + 15 \frac{f^4}{g^4} \log \left(1 + \frac{g}{f} \right) - f^4 \frac{11g+10f}{2g^3 \cdot (g+f)^2} \right] \\ F_{04} &= \frac{g^2+3gf+3f^2}{3f^3 \cdot (g+f)^3} \\ F_{14} &= \frac{g+3f}{6f^2 \cdot (g+f)^3} \end{aligned} \quad (\text{C.5})$$

$$\begin{aligned}
F_{24} &= \frac{1}{3f \cdot (g+f)^3} \\
F_{34} &= \frac{1}{g^3} \cdot \left[\frac{1}{g} \log \left(1 + \frac{g}{f} \right) - \frac{11g^2 + 15gf + 6f^2}{6 \cdot (g+f)^3} \right] \\
F_{44} &= \frac{1}{g^4} \cdot \left[1 - 4\frac{f}{g} \log \left(1 + \frac{g}{f} \right) + f \frac{13g^2 + 21gf + 9f^2}{3 \cdot (g+f)^3} \right] \\
F_{25} &= \frac{g+4f}{12f^2 \cdot (g+f)^4} \\
F_{35} &= \frac{1}{4f \cdot (g+f)^4} \\
F_{45} &= \frac{1}{g^4} \cdot \left[\frac{1}{g} \log \left(1 + \frac{g}{f} \right) - \frac{25g^3 + 52g^2f + 42gf^2 + 12f^3}{12 \cdot (g+f)^4} \right] \\
F_{55} &= \frac{1}{g^5} \cdot \left[1 - 5\frac{f}{g} \log \left(1 + \frac{g}{f} \right) + f \frac{77g^3 + 188g^2f + 162gf^2 + 48f^3}{12 \cdot (g+f)^4} \right].
\end{aligned}$$

Acknowledgements

We wish to thank M.Göckeler, H.Perlt and G.Schierholz for communicating to us their results prior to publication, and for many useful discussions. We also thank M. Ciuchini, E. Franco and M. Testa for comments and discussions.

References

- [1] S.Capitani and G.C.Rossi, Nucl. Phys. **B433** (1995) 351
- [2] K.Symanzik, in “Mathematical Problems in Theoretical Physics”, Springer Lecture Notes in Physics, vol. **153** (1982) 47 (R.Schrader, R.Seiler and D.A.Uhlenbrock eds.)
- [3] M.Lüscher and P.Weisz, Commun. Math. Phys. **97** (1985) 59
- [4] B.Sheikholeslami and R.Wohlert, Nucl. Phys. **B259** (1985) 572
- [5] G.Heatlie, G.Martinelli, C.Pittori, G.C.Rossi and C.T.Sachrajda, Nucl. Phys. **B352** (1991) 266 and Nucl. Phys. **B** (Proc. Suppl.) **17** (1990) 607; E.Gabrielli, G.Heatlie, G.Martinelli, C.Pittori, G.C.Rossi, C.T.Sachrajda and A.Vladikas, Nucl. Phys. **B** (Proc. Suppl.) **20** (1991) 448
- [6] G.Altarelli, Phys. Rep. **81** (1982) 1
- [7] D.J.Gross, in “Methods in field theory”, Les Houches, Session XXVIII, 1975, North-Holland (1976) 141 (R.Balian and J.Zinn-Justin eds.)

- [8] D.J.Gross and F.Wilczek, Phys. Rev. **D8** (1973) 3633 and Phys. Rev. **D9** (1974) 980
- [9] H.Georgi and H.D.Politzer, Phys. Rev. **D9** (1974) 416
- [10] N.Christ, B.Hasslacher and A.Mueller, Phys. Rev. **D6** (1972) 3543
- [11] K.G.Wilson, Phys. Rev. **D10** (1974) 2445 and in “New Phenomena in Subnuclear Physics”, Plenum Press, New York (1977) (A.Zichichi ed.)
- [12] M.Baake, B.Gemünden and R.Oedingen, Journ. Math. Phys. **23** (1982) 944
- [13] J.Mandula, G.Zweig and J.Govaerts, Nucl. Phys. **B228** (1983) 91
- [14] G.Martinelli and C.T.Sachrajda, Phys. Lett. **B196** (1987) 184 and Nucl. Phys. **B306** (1988) 865
- [15] G.Martinelli and C.T.Sachrajda, Nucl. Phys. **B316** (1989) 355
- [16] M.Göckeler, R.Horsley, M.Ilgenfritz, H.Perlt, P.Rakov, G.Schierholz and A.Schiller, in preparation
- [17] S.Capitani and G.C.Rossi, Rome “Tor Vergata” Preprint ROM2F/95/06, to be published in the Proceedings of the IV AIHENP95 International Workshop, World Scientific Ed.
- [18] S.Capitani, Ph.D. Thesis, Univ. of Rome “La Sapienza”, Rome, 1994
- [19] G.Beccarini, Undergraduate Thesis, Univ. of L’Aquila, L’Aquila, 1993
- [20] M.Göckeler, R.Horsley, M.Ilgenfritz, H.Perlt, P.Rakov, G.Schierholz and A.Schiller, in preparation
- [21] M.Göckeler, R.Horsley, M.Ilgenfritz, H.Perlt, P.Rakov, G.Schierholz and A.Schiller, Nucl. Phys. **B** (Proc. Suppl.) **42** (1995) 337